Transient characteristics of chaos synchronization in a semiconductor laser subject to optical feedback

A. Uchida, N. Shibasaki, S. Nogawa, and S. Yoshimori
Department of Electronics and Computer Systems, Takushoku University, 815-1 Tatemachi, Hachioji, Tokyo 193-0985, Japan
(Received 29 July 2002; revised manuscript received 9 January 2004; published 4 May 2004)

We have investigated the transient characteristics of two types of chaos synchronization in a semiconductor laser subject to optical feedback: complete synchronization and strong injection locking-type synchronization. We have calculated the statistical distribution of the transient response time of synchronization when the initial position in the starting attractor is varied. For complete synchronization, the distribution of the transient response time has much larger average and variance than the average period of the chaotic oscillations. Conversely, a short transient response time is obtained for strong injection locking-type synchronization. We found that the transient response time is dependent upon the maximum Lyapunov exponent of the chaotic temporal waveform for complete synchronization, whereas it is almost constant for strong injection locking-type synchronization.

DOI: 10.1103/PhysRevE.69.056201 PACS number(s): 05.45.Xt, 42.65.Sf, 42.55.Px

I. INTRODUCTION

Synchronization of chaos has attracted increasing interest for applications of secure communications [1,2]. One of the communication methods using chaos is called chaos shift keying, in which two chaotic attractors are treated as two binary codes for the transmission of digital information [3]. Chaotic on-off keying is a simple version of the chaos shift keying, in which two different values of the accuracy of synchronization are used to distinguish two binary codes [4]. In these communication schemes, the transient response time of chaos synchronization has to be shortened for higher transmission rates. However, the transient characteristics of chaos synchronization have not been investigated so far.

The transient characteristics from chaos to controlled periodic states have been investigated in the Henon map and CO_2 lasers [5–7]. The switching between two controlled periodic attractors has also been investigated in a semiconductor laser [8]. In these studies, the transient response time is dependent upon the initial attractor, and its probability distribution is of an exponential nature, which is called "chaotic transient" [5]. Switching characteristics between different attractors are also important in understanding the dynamics of low frequency fluctuations (LFF) in semiconductor lasers that are subject to optical feedback [9]. LFF is an abrupt power-dropout event in laser output over a long time scale when compared with the relaxation oscillation period. Such a phenomenon has been attributed to chaotic itinerancy or spontaneous switching behavior between unstable attractors. These switching characteristics are similar to the transient dynamics between periodic attractors stabilized from chaotic attractors [8]. However, the studies on transient characteristics of chaos synchronization have not been reported in laser systems.

In this study, we investigate the transient characteristics of chaos synchronization in a semiconductor laser subject to optical feedback. There are two types of chaos synchronization in a semiconductor laser with optical feedback, which are called complete synchronization and strong injection locking-type synchronization [10–16]. The main difference of the two types is a time delay between the two chaotic wave forms. Complete synchronization of electrical amplitudes between the master laser E_m and the slave laser E_s can be denoted as $E_s(t)=E_m(t-\tau_{inj}+\tau_m)$, where the delay between the two lasers is dependent on both a delay of external feedback light in the master laser τ_m and a delay of injection signal from the master to the slave lasers τ_{inj}. Since the complete synchronization corresponds to a mathematical solution of synchronization in Lang-Kobayashi equations, all the parameters must be set to be identical. This synchronization has been also known as anticipating chaos [17–19], when τ_m is greater than τ_{inj}. On the other hand, there is another type of synchronization, which is called strong injection locking-type synchronization (also called conventional synchronization [13], time lag synchronization [15], and synchronization by amplification [16]). In this case, the delay between the two lasers is only dependent on τ_{inj} and the amplitudes of the two chaotic wave forms are different, i.e., $E_s(t)=A\times E_m(t-\tau_{inj})$. Strong injection locking effect induces this type of synchronization. In this paper, we calculate the transient time for both of the two types of synchronization and clarify differences between them. We also investigate the relationship between the transient response time and the maximum Lyapunov exponent of injected chaotic wave forms.

II. MODEL

Figure 1 shows our numerical model. A compound cavity of a single-longitudinal-mode semiconductor laser is used as a master laser, where the laser is subject to external feedback light from an external mirror. The laser light is reflected by the external mirror located at a distance L from the front facet of the cavity of the semiconductor laser. The output of the master laser is injected into the cavity of a slave laser without external feedback for chaos synchronization. We change the strength of the injection beam to demonstrate the two types of chaos synchronization. The amplitude of feed-

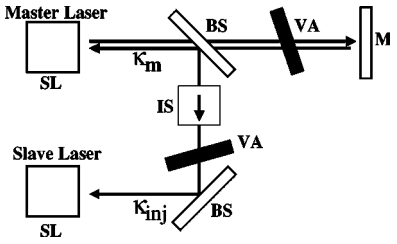

FIG. 1. Numerical model of chaos synchronization in two semiconductor lasers. BS: beam splitter, IS: optical isolator, *M*: mirror, SL: semiconductor laser, VA: variable attenuator, κ_m: feedback coefficient of the master laser, κ_{inj}: injection coefficient from the master to the slave laser.

back light is varied by changing the reflectivity of the external mirror r_3.

The Lang-Kobayashi equations have been used for two decades to describe the dynamics of a single-longitudinal-mode semiconductor laser with weak optical feedback [20,21]. However, a limit of validity of the Lang-Kobayashi equations for a Fabry-Perot laser has been pointed out that the description of the laser with optical feedback requires a multilongitudinal model even in the presence of tiny amount of optical feedback [22,23]. In our calculation, we assume a distributed-feedback (DFB) semiconductor laser to avoid multi-longitudinal-mode oscillations all the time. Under this condition, the Lang-Kobayashi equations are reasonable to describe the dynamics of a semiconductor laser subject to optical feedback [12,24]. The Lang-Kobayashi equations are described as follows:

Master laser:

$$\frac{dE_m(t)}{dt} = \frac{1}{2}\left\{G_N[N_m(t) - N_0] - \frac{1}{\tau_p}\right\}E_m(t) + \frac{\kappa_m}{\tau_{in}}E_m(t-\tau_m)\cos[\Delta_m(t)], \quad (2.1)$$

$$\frac{d\Phi_m(t)}{dt} = \frac{\alpha}{2}G_N[N_m(t) - N_{th}] - \frac{\kappa_m E_m(t-\tau_m)}{\tau_{in}E_m(t)}\sin[\Delta_m(t)], \quad (2.2)$$

$$\frac{dN_m(t)}{dt} = J - \frac{N_m(t)}{\tau_s} - G_N[N_m(t) - N_0]|E_m(t)|^2, \quad (2.3)$$

$$\Delta_m(t) = \omega_m\tau_m + \Phi_m(t) - \Phi_m(t-\tau_m). \quad (2.4)$$

Slave laser:

$$\frac{dE_s(t)}{dt} = \frac{1}{2}\left\{G_N[N_s(t) - N_0] - \frac{1}{\tau_p}\right\}E_s(t) + \frac{\kappa_{inj}}{\tau_{in}}E_m(t-\tau_{inj})\cos[\Delta_s(t)], \quad (2.5)$$

$$\frac{d\Phi_s(t)}{dt} = \frac{\alpha}{2}G_N[N_s(t) - N_{th}] - \frac{\kappa_{inj}E_m(t-\tau_{inj})}{\tau_{in}E_s(t)}\sin[\Delta_s(t)], \quad (2.6)$$

$$\frac{dN_s(t)}{dt} = J - \frac{N_s(t)}{\tau_s} - G_N[N_s(t) - N_0]|E_s(t)|^2, \quad (2.7)$$

$$\Delta_s(t) = -\Delta\omega t + \omega_m\tau_{inj} + \Phi_s(t) - \Phi_m(t-\tau_{inj}), \quad (2.8)$$

where $E(t)$ and $\Phi(t)$ are the electrical amplitude and the phase, $N(t)$ is the carrier density, and $\Delta(t)$ is the phase difference. The subscripts m,s indicate the master and slave lasers. G_N is the gain coefficient, N_0 is the carrier density at the transparency, $N_{th}=N_0+1/(G_N\tau_p)$ is the threshold of carrier density for the solitary laser, $\kappa_m=(1-r_2^2)r_3/r_2$ is the feedback coefficient of the master laser, r_2 is the facet reflectivity of electrical amplitude, r_3 is the reflectivity of the external mirror of electrical amplitude, and κ_{inj} is the injection coefficient. τ_p is the photon lifetime, $\tau_{in}=2nl/c$ is the optical round-trip time in the cavity of the semiconductor laser, l is the cavity length, n is the refractive index, τ_s is the carrier lifetime, $\tau_m=2nL/c$ is the round trip time of the external cavity in the master laser, τ_{inj} is the transmission time of injection signal from the master to the slave laser, α is the linewidth enhancement factor, J is the injection current density, and $J_{th}=N_{th}/\tau_s$ is the threshold of the injection current density. $\omega_m=2\pi c/\lambda_m$ is the angular frequency of the master laser, λ_m is the wavelength of the master laser, $\Delta\omega=\omega_m-\omega_s$ is the detuning of the angular frequencies between the master and slave lasers. The coupling from the master to the slave laser is introduced via the term of $E_m(t-\tau_{inj})$ in Eqs. (2.5) and (2.6). We ignore the small contribution from nonlinear gain suppression and spontaneous emission. Since the amount of feedback light relative to the output power of lasers is very small (10^{-4}–10^{-5}), secondary optical feedback is negligible. In our calculation, the Langevin noise terms are ignored for the sake of simplicity. All the parameters are set to be identical between the master and slave lasers except κ_m and κ_{inj}, as shown in Table I. We numerically integrate Eqs. (2.1)–(2.8) by employing the Runge-Kutta-Gill method.

III. NUMERICAL CALCULATION

A. Complete synchronization

We focus on the transient response time for complete synchronization in this section. All the parameters are set to be identical between the master and slave lasers. In particular, the condition for complete synchronization is satisfied as $\kappa_m=\kappa_{inj}$ and $\tau_m=\tau_{inj}$ [10].

We investigate the transient response time when the output of the master laser is injected into the slave laser in a step-function. The transient response time is defined as the time from the beginning of the step function to the moment at which the intensity level of the slave laser reaches a region within 10 % of the asymptotic values of the master laser, as shown in Fig. 2. We calculate the difference of two temporal wave forms at each point for whole time series, and the

TABLE I. Parameter values for semiconductor lasers used in our calculations.

Symbol	Parameter	Value
G_N	Gain coefficient	8.4×10^{-13} m^3s^{-1}
N_0	Carrier density at transparency	1.4×10^{24} m^{-3}
N_{th}	Carrier density at threshold	2.018×10^{24} m^{-3}
τ_p	Photon lifetime	1.927 ps
τ_{in}	Round-trip time in laser cavity	8.0 ps
τ_s	Carrier lifetime	2.04 ns
τ_m	Round-trip time in the external cavity	3.33 ns
τ_{inj}	Transmission time of injection signal	3.33 ns
α	Linewidth enhancement factor	3.0
J	Injection current density	1.1 J_{th}
J_{th}	Threshold of injection current density	9.89×10^{32} m^{-3} s^{-1}
λ_m	Wavelength of master laser	1537 nm
$\Delta\omega$	Detuning angular frequency	0
r_2	Facet reflectivity	0.556
r_3	Reflectivity of external mirror	Variable
κ_m	Feedback coefficient	Variable
κ_{inj}	Injection coefficient	Variable

transient response time is defined as the latest time at which the difference converges and remains within 10% for the rest of the time series.

According to our calculations, the transient response time for chaos synchronization is greatly influenced by its initial position in the starting attractor before switching occurs. These results coincide well with the transition characteristics between stabilized periodic attractors in Ref. [8]. Therefore, we calculate the statistical distribution of the transient response time when the initial position in the starting attractor is varied for 5000 points. We select the initial conditions uniformly on the chaotic attractors, and the way of selecting initial conditions does not affect the distribution of transient response time when a large number of initial positions more than 5000 points are used.

Figure 3 shows the statistical distributions of the transient response time for chaos synchronization [Figs. 3(a), 3(b) and 3(c)] and examples of temporal wave forms of the two lasers including the transient process [Figs. 3(d), 3(e) and 3(f)] at various r_3. As r_3 is increased, the distributions have large average transient response times and large variances. The average transient response time deduced from Fig. 3 can be given for each of the synchronized states as (a) 14 ns, (b) 71 ns, and (c) 182 ns, where the average period of the chaotic oscillations is 1.45 ns. These average transient response times for complete synchronization are much longer than the average period of the chaotic oscillations.

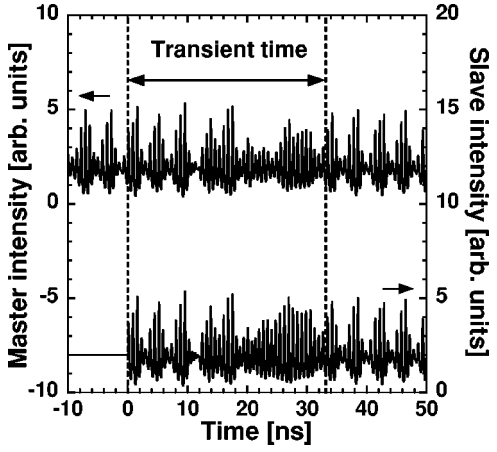

FIG. 2. Typical example of chaotic temporal wave forms and the definition of the transient response time of chaos synchronization.

We calculate the average transient response time when the reflectivity of the external mirror r_3 is continuously changed, as shown in Fig. 4(a). The average transient response time is increased as r_3 is increased. Figure 4(b) shows the bifurcation diagram of the temporal wave forms of the master laser as a function of r_3, corresponding to Fig. 4(a). The bifurcation diagram is obtained by sampling peak values of temporal wave forms after transient process at various r_3. At weak reflectivity of r_3 less than 0.004 75, quasiperiodic oscillations are observed and the average transient response time has a small value less than 5 ns. In this condition, the transient response time is not dependent upon initial conditions. As the temporal wave forms are changed to be more chaotic with increase of r_3, the average transient response time increases. Therefore, the characteristics of temporal wave forms are important in determining the average transient response time.

To investigate the dependence of the characteristics of chaotic wave forms upon the transient response time, we calculate the maximum Lyapunov exponent of chaotic temporal wave forms of the master laser at various r_3. We evaluate the variational equations for the master laser derived from Eqs. (2.1)–(2.4) along the trajectory in the phase space [25–28]. The variational equations are obtained from the linearization of Eqs. (2.1)–(2.4) and are described as follows:

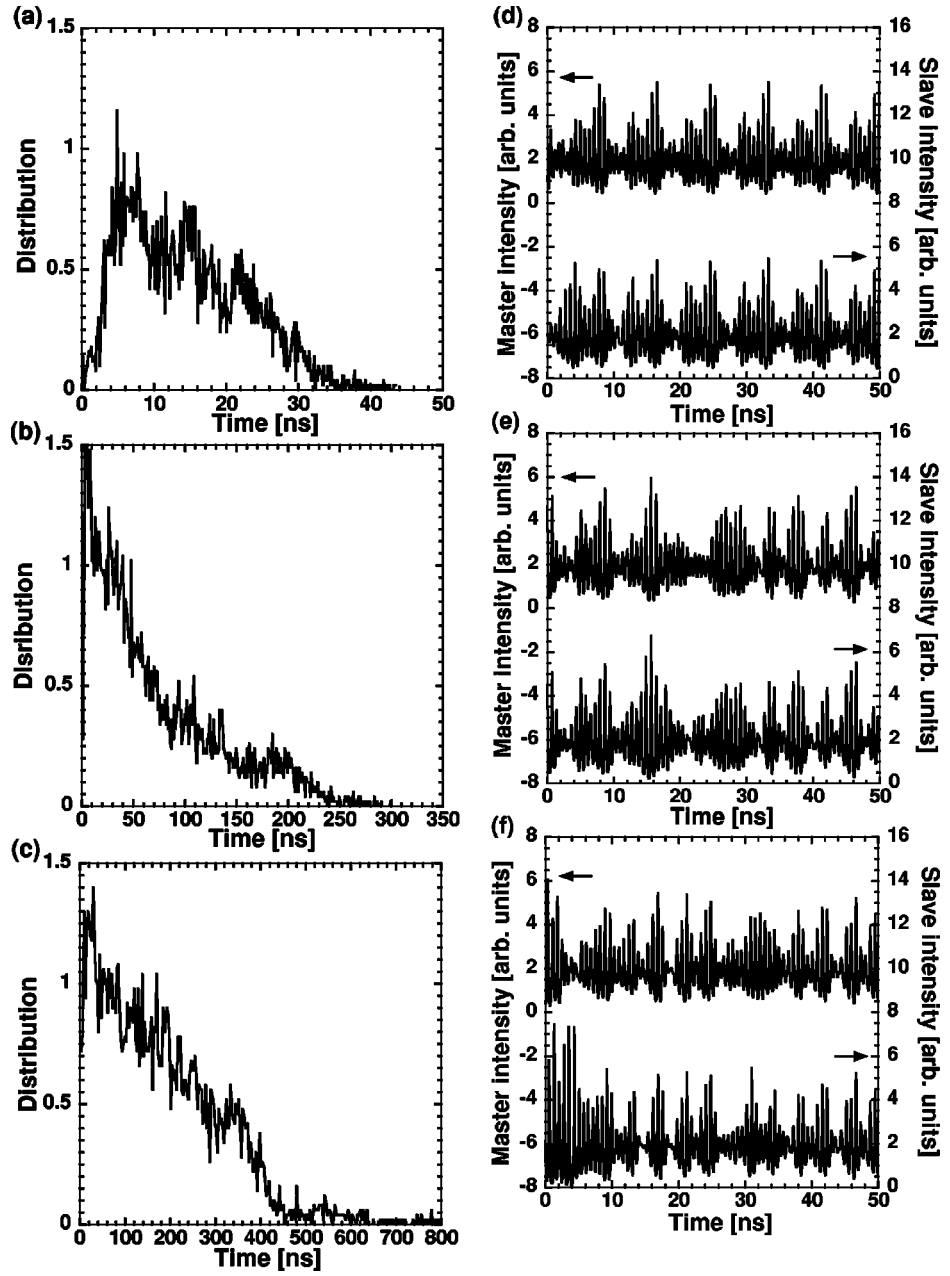

FIG. 3. Statistical distributions of the transient response time [(a),(b),(c)] and examples of temporal wave forms of the two lasers including transient process [(d),(e),(f)] at three values of the reflectivity of the external mirror r_3 for complete synchronization. (a),(d) $r_3=0.0050$, (b),(e) $r_3=0.0055$, and (c),(f) $r_3=0.0060$. All of the temporal wave forms in (d), (e), and (f) exhibit chaotic dynamics. Note that the scales of the horizontal axes in (a), (b), and (c) are different.

$$\frac{de(t)}{dt}=\frac{1}{2}\left\{G_N[N_m(t)-N_0]-\frac{1}{\tau_p}\right\}e(t) - \frac{\kappa_m}{\tau_{in}}E_m(t-\tau_m)\sin[\Delta_m(t)]\delta(t)+\frac{1}{2}G_N E_m(t)n(t) + \frac{\kappa_m}{\tau_{in}}\cos[\Delta_m(t)]e(t-\tau_m). \tag{3.1}$$

$$\frac{d\delta(t)}{dt}=\frac{\kappa_m}{\tau_{in}}\frac{E_m(t-\tau_m)}{|E_m(t)|^2}\sin[\Delta_m(t)]e(t) - \frac{\kappa_m}{\tau_{in}}\frac{E_m(t-\tau_m)}{E_m(t)}\cos[\Delta_m(t)]\delta(t)+\frac{\alpha}{2}G_N n(t) - \frac{\kappa_m}{\tau_{in}}\frac{1}{E_m(t)}\sin[\Delta_m(t)]e(t-\tau_m). \tag{3.2}$$

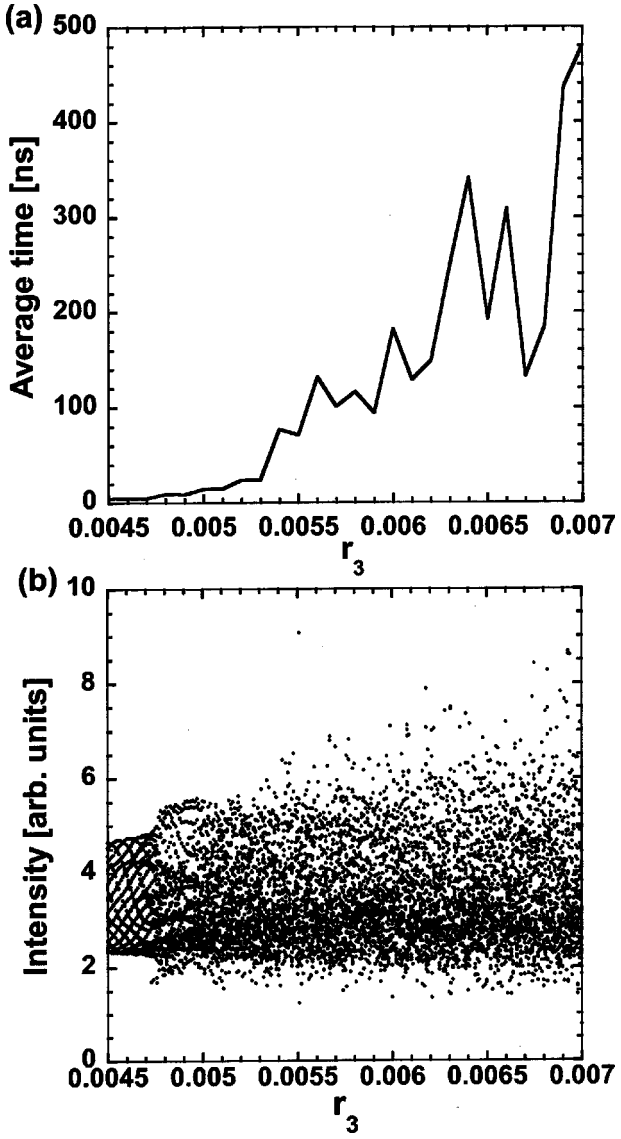

FIG. 4. (a) Average transient response time as a function of r_3 for complete synchronization. (b) Bifurcation diagram of temporal waveform of the master laser as a function of r_3.

$$\frac{dn(t)}{dt} = -2G_N E_m(t)[N_m(t) - N_0]e(t) - \left(G_N|E_m(t)|^2 + \frac{1}{\tau_s}\right)n(t). \tag{3.3}$$

Where, $e(t)$, $\delta(t)$, and $n(t)$ are the linearized variables of $E_m(t)$, $\Delta_m(t)$, and $N_m(t)$. These three linearized variables are calculated along the trajectory of $[E_m(t), \Delta_m(t), N_m(t)]$ obtained from Eqs. (2.1)–(2.4) in the phase space. The norm of the linearized variables $D(t)$ is defined as

$$D(t) = \sqrt{|e(t)|^2 + |\delta(t)|^2 + |n(t)|^2}. \tag{3.4}$$

After a short evolution of the trajectory τ_{ev}, the variation of the norms d is calculated as

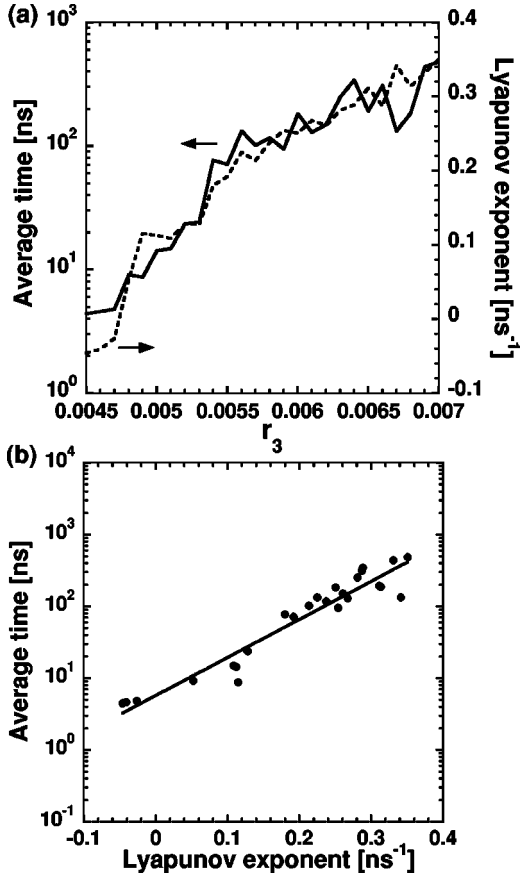

FIG. 5. (a) Average transient response time in the logarithmic scale (solid curve) and the maximum Lyapunov exponent of the master-laser output (dotted curve) as a function of r_3 for complete synchronization. (b) Relationship between the maximum Lyapunov exponent and the average transient response time in the semi-logarithmic plot.

$$d_i = \frac{D(t + \tau_{ev})}{D(t)}. \tag{3.5}$$

Where d_i is the ratio of the norms after the short evolution τ_{ev} at the ith procedure of the above calculation. Next, all the variations of $e(t)$, $\delta(t)$, and $n(t)$ are rescaled by $D(t+\tau_{ev})$ and integration of the trajectory resumes for the next evolution of τ_{ev}. After this procedure is repeated N times, the maximum Lyapunov exponent is calculated as

$$\lambda = \frac{1}{N\tau_{ev}} \sum_{i}^{N} \ln(d_i). \tag{3.6}$$

The maximum Lyapunov exponent can be obtained as the average ratio of norm change in the logarithmic scale. In this procedure, we essentially calculate the Jacobian matrix of the original equations along the trajectory of the attractor and evaluate the growth of perturbation from the original trajectory. Therefore, the estimation of the maximum Lyapunov exponent by using variational equations is very reliable compared with the estimation based on time series analysis.

Figure 5(a) shows the average transient response time (in the logarithmic scale) and the maximum Lyapunov exponent

of the master-laser output as a function of r_3. The shape of the two curves correlates with each other as shown in Fig. 5(a). Figure 5(b) shows the relationship between the maximum Lyapunov exponent and the average transient response time. This figure clearly shows that there is a linear correlation between the maximum Lyapunov exponent and the average transient response time in the semilogarithmic plot. Therefore, the transient response time is strongly dependent upon the characteristics of chaos for complete synchronization. Longer transient response times are required for more complicated chaotic wave forms (i.e., larger maximum Lyapunov exponent) for complete synchronization.

B. Complete synchronization with external feedback

In this section, we change the configuration of our model in Fig. 1. We set an external mirror in front of the slave laser to introduce self-feedback light and investigate the transient response time as a function of r_3. The rate equations for the slave laser shown in Eqs. (2.5)–(2.8) are modified as follows:

Slave laser:

$$\frac{dE_s(t)}{dt} = \frac{1}{2}\left\{ G_N[N_s(t) - N_0] - \frac{1}{\tau_p} \right\} E_s(t) + \frac{\kappa_{inj}}{\tau_{in}} E_m(t - \tau_{inj}) \times \cos[\Delta_s(t)] + \frac{\kappa_s}{\tau_{in}} E_s(t - \tau_{sl}) \cos[\Delta_{s,ext}(t)]. \quad (3.7)$$

$$\frac{d\Phi_s(t)}{dt} = \frac{\alpha}{2} G_N[N_s(t) - N_{th}] - \frac{\kappa_{inj} E_m(t - \tau_{inj})}{\tau_{in} E_s(t)} \sin[\Delta_s(t)] - \frac{\kappa_s E_s(t - \tau_{sl})}{\tau_{in} E_s(t)} \sin[\Delta_{s,ext}(t)]. \quad (3.8)$$

$$\frac{dN_s(t)}{dt} = J - \frac{N_s(t)}{\tau_s} - G_N[N_s(t) - N_0]|E_s(t)|^2. \quad (3.9)$$

$$\Delta_s(t) = -\Delta\omega t + \omega_m \tau_{inj} + \Phi_s(t) - \Phi_m(t - \tau_{inj}). \quad (3.10)$$

$$\Delta_{s,ext}(t) = \omega_s \tau_{sl} + \Phi_s(t) - \Phi_s(t - \tau_{sl}). \quad (3.11)$$

Where κ_s is the feedback coefficient of the slave laser, τ_{sl} is the round-trip time of the external cavity in the slave laser. To maintain the complete synchronization, the feedback coefficient of the master laser κ_m is set to be equal to the sum of the injection coefficient into the slave laser κ_{inj} and the feedback coefficient of the slave laser κ_s, i.e., $\kappa_m = \kappa_{inj} + \kappa_s$. We set $\kappa_{inj} = 0.8\ \kappa_m$ and $\kappa_s = 0.2\kappa_m$ to satisfy this condition. The delay times of the external feedback for the master and slave lasers and the transmission time of the injection signal are set to be identical ($\tau_m = \tau_{sl} = \tau_{inj}$). We calculate the transient response time by integrating Eqs. (2.1)–(2.4) for the master laser and Eqs. (3.7)–(3.11) for the slave laser.

Figure 6 shows the distributions of the transient response time at various r_3. Comparing with Figs. 3(a), 3(b) and 3(c), the average transient response times of the distributions are enlarged due to the self-feedback in the slave laser. A large transient is required to suppress its own chaotic dynamics in the slave laser. Figure 7(a) shows the average transient response time and the maximum Lyapunov exponent of the master-laser output as a function of r_3. It is worth noting that the average transient response times are larger than those in Fig. 5(a). This result shows the transient response time increases in the presence of the self-feedback light from the external mirror in the slave laser for complete synchronization. We also investigate the relationship between the average transient response time and the maximum Lyapunov exponent as shown in Fig. 7(b). It is found that the average transient response time and the maximum Lyapunov expo-

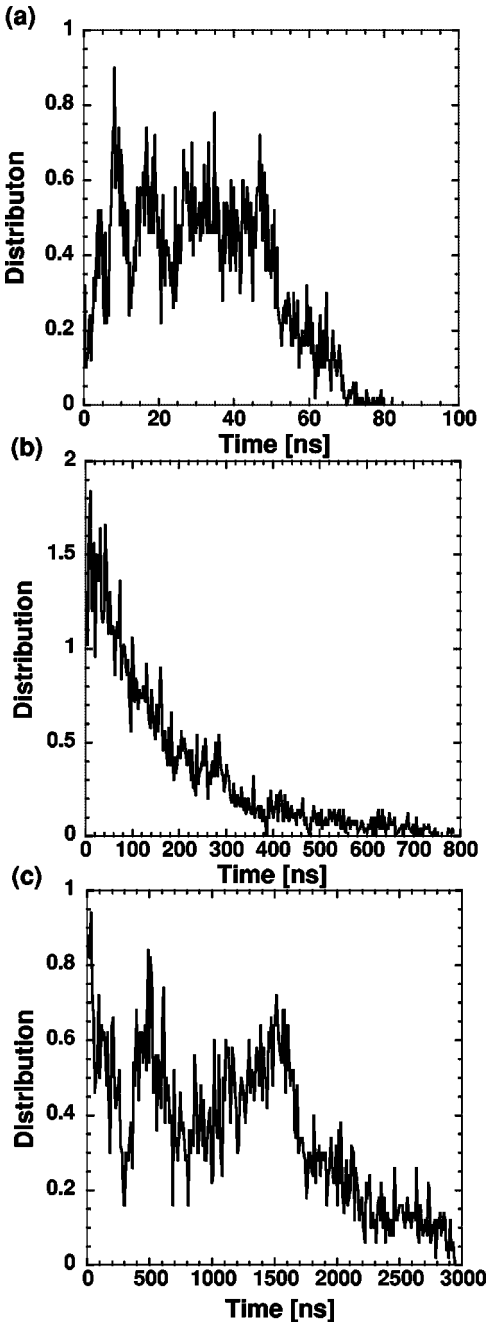

FIG. 6. Statistical distributions of the transient response time at three values of the reflectivity of the external mirror r_3 for complete synchronization of the slave laser with self-feedback light. (a) $r_3 = 0.0050$, (b) $r_3 = 0.0055$, and (c) $r_3 = 0.0060$. Note that the scales of the horizontal axes in (a),(b),(c) are different.

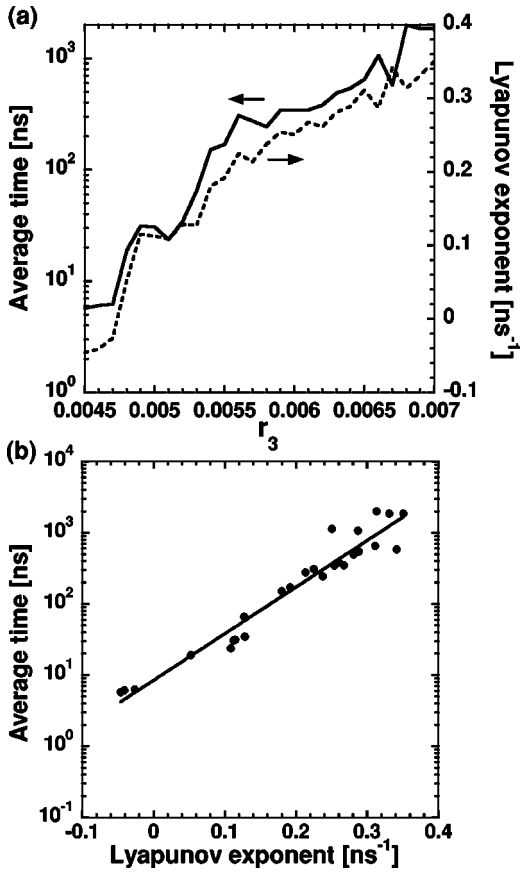

FIG. 7. (a) Average transient response time in the logarithmic scale (solid curve) and the maximum Lyapunov exponent of the master-laser output (dotted curve) as a function of r_3 for complete synchronization of the slave laser with self-feedback light. (b) Relationship between the maximum Lyapunov exponent and the average transient response time in the semilogarithmic plot.

nent of chaotic wave forms are linearly correlated in the semi-logarithmic plot, as well in the case of Fig. 5(b). However, the slope of the line of best fit in Fig. 7(b) is larger than that in Fig. 5(b), due to the presence of self-feedback light in the slave laser.

C. Strong injection locking-type synchronization

When the injection coefficient κ_{inj} is increased, a different type of chaos synchronization can be observed, which is referred to as strong injection locking-type synchronization [10–16]. In this case, the chaotic oscillations are simply amplified in the slave laser by using the injection locking effect, where the frequency of optical carrier can be matched between two coupled lasers [29]. We investigate the transient response time of the injection locking-type synchronization. We set the coupling coefficient as $\kappa_{inj}=100\kappa_m$ to achieve injection locking-type synchronization. We remove the external mirror in the slave laser in this configuration ($\kappa_s=0$), i.e., we integrate Eqs. (2.1)–(2.8) to calculate the transient response time for strong injection locking-type synchronization.

Figure 8 shows the distributions of the transient response time for the injection locking-type synchronization at three

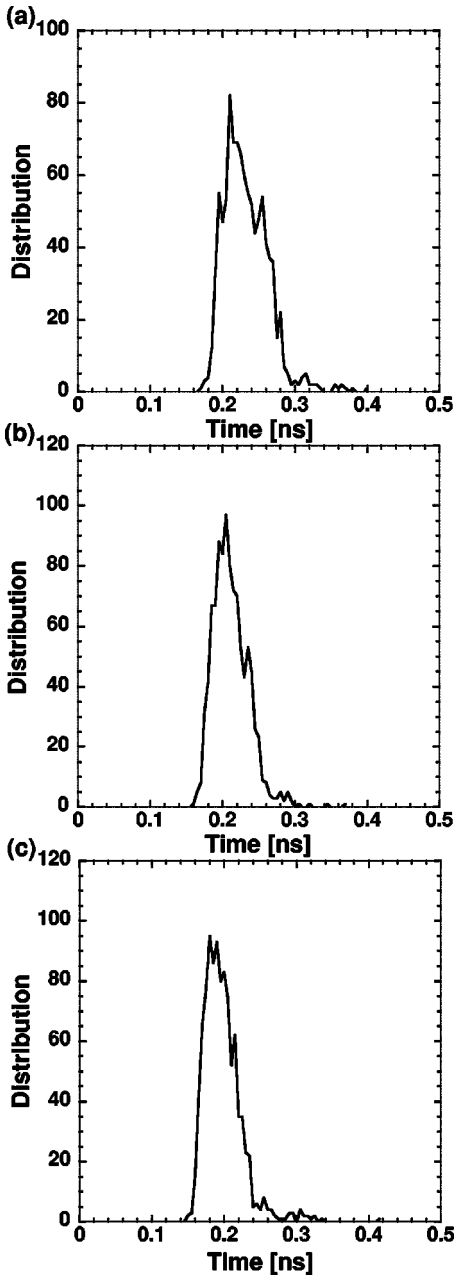

FIG. 8. Statistical distributions of the transient response time at three values of the reflectivity of the external mirror r_3 for strong injection locking-type synchronization. (a) $r_3=0.0050$, (b) $r_3=0.0055$, and (c) $r_3=0.0060$.

different values of r_3. It is significant that all the distributions have a similar shape, and the average transient response time (0.21 ns) is much shorter than that for the complete synchronization. Figure 9(a) shows the average transient response time and the maximum Lyapunov exponent of the master-laser output as a function of r_3. The average transient response time is within one period of the chaotic temporal wave forms (1.45 ns) for all r_3. The transient process of synchronization is very fast because chaotic oscillations are amplified in the slave laser due to the strong injection from the master laser, regardless of the characteristics of chaotic temporal wave forms. Figure 9(b) shows the relationship be-

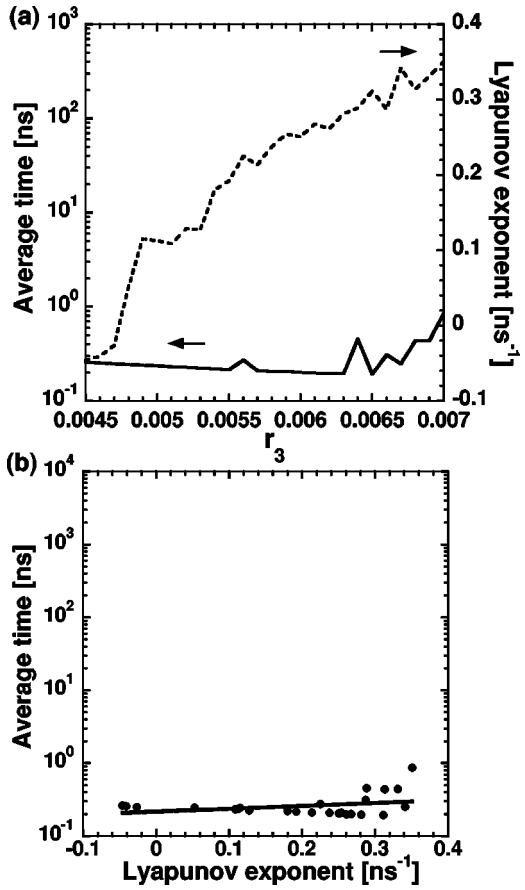

FIG. 9. (a) Average transient response time in the logarithmic scale (solid curve) and the maximum Lyapunov exponent of the master-laser output (dotted curve) as a function of r_3 for strong injection locking-type synchronization. (b) Relationship between the maximum Lyapunov exponent and the average transient response time in the semilogarithmic plot.

tween the average transient response time and the maximum Lyapunov exponent. The average transient response time is almost constant as the maximum Lyapunov exponent is changed. We found that the transient response time is not dependent upon the characteristics of chaotic wave forms for strong injection locking-type synchronization.

It turns out that the transient characteristics of the two types of chaos synchronization are totally different. The measurement of the transient response time is a new method to distinguish the two types of chaos synchronization in a semiconductor laser subject to optical feedback, instead of the measurement of a time lag between the two chaotic wave forms [12]. From the applications point of view, the injection locking-type synchronization is preferable for communications using laser chaos because it can avoid the long transient process of synchronization for chaos shift keying and chaotic on-off keying methods.

IV. CONCLUSION

We have investigated the transient characteristics of the two types of chaos synchronization in a semiconductor laser subject to optical feedback: complete synchronization and strong injection locking-type synchronization. We have calculated the statistical distribution of the transient response time when the initial position in the starting attractor is varied. For complete synchronization, the distribution of the transient response time has a much larger average and variance than the average period of the chaotic oscillations. The average transient response time becomes large as the maximum Lyapunov exponent of the injected chaotic wave form is increased. When the slave laser has an external mirror, the transient response time is larger than that without external mirror. Conversely, short transient response time is obtained for strong injection locking-type synchronization. We found that the transient response time is dependent upon the maximum Lyapunov exponent of the chaotic temporal wave form for complete synchronization, whereas it is almost constant for strong injection locking-type synchronization.

ACKNOWLEDGMENTS

We thank Peter Davis, Louis Pecora, and Rajarshi Roy for helpful discussions. This work was financially supported by The Sumitomo Foundation, the Telecommunications Advancement Foundation, a Sasakawa Scientific Research Grant from the Japan Science Society, the Promotion and Mutual Aid Corporation for Private Schools of Japan, and a Grant-in-Aid for Encouragement of Young Scientists from the Japan Society for the Promotion of Science.

[1] G. D. VanWiggeren and R. Roy, Science **279**, 1198 (1998).
[2] J.-P. Goedgebuer, L. Larger, and H. Porte, Phys. Rev. Lett. **80**, 2249 (1998).
[3] J.-B. Cuenot, L. Larger, J.-P. Goedgebuer, and W. T. Rhodes, IEEE J. Quantum Electron. **37**, 849 (2001).
[4] A. Uchida, S. Yoshimori, M. Shinozuka, T. Ogawa, and F. Kannari, Opt. Lett. **26**, 866 (2001).
[5] C. Grebogi, E. Ott, and J. A. Yorke, Phys. Rev. Lett. **57**, 1284 (1986).
[6] T. Tel, J. Phys. A **24**, L1359 (1991).
[7] R. Meucci, W. Gadomski, M. Ciofini, and F. T. Arecchi, Phys. Rev. E **52**, 4676 (1995).
[8] A. Uchida, T. Sato, T. Ogawa, and F. Kannari, IEEE J. Quantum Electron. **35**, 1374 (1999).
[9] D. W. Sukow, J. R. Gardner, and D. J. Gauthier, Phys. Rev. A **56**, R3370 (1997).
[10] V. Ahlers, U. Parlitz, and W. Lauterborn, Phys. Rev. E **58**, 7208 (1998).
[11] Y. Liu, H. F. Chen, J. M. Liu, P. Davis, and T. Aida, Phys. Rev. A **63**, 031802(R) (2001).
[12] Y. Liu, Y. Takiguchi, P. Davis, T. Aida, S. Saito, and J. M. Liu, Appl. Phys. Lett. **80**, 4306 (2002).

[13] A. Locquet, F. Rogister, M. Sciamanna, P. Megret, and M. Blondel, Phys. Rev. E **64**, 045203(R) (2001).
[14] A. Locquet, C. Masoller, P. Megret, and M. Blondel, Opt. Lett. **27**, 31 (2002).
[15] I. V. Koryukin and P. Mandel, Phys. Rev. E **65**, 026201 (2002).
[16] A. Murakami and J. Ohtsubo, Phys. Rev. A **65**, 033826 (2002).
[17] H. U. Voss, Phys. Rev. E **61**, 5115 (2000).
[18] C. Masoller, Phys. Rev. Lett. **86**, 2782 (2001).
[19] S. Sivaprakasam, E. M. Shahverdiev, P. S. Spencer, and K. A. Shore, Phys. Rev. Lett. **87**, 154101 (2001).
[20] R. Lang and K. Kobayashi, IEEE J. Quantum Electron. **16**, 347 (1980).
[21] Y. Liu, N. Kikuchi, and J. Ohtsubo, Phys. Rev. E **51**, R2697 (1995).
[22] A. A. Duarte and H. G. Solari, Phys. Rev. A **58**, 614 (1998).
[23] A. A. Duarte and H. G. Solari, Phys. Rev. A **60**, 2403 (1999).
[24] V. Annovazzi-Lodi, S. Merlo, M. Norgia, and A. Scire, IEEE J. Quantum Electron. **38**, 1171 (2002).
[25] L. M. Pecora and T. L. Carroll, Phys. Rev. Lett. **64**, 821 (1990).
[26] L. M. Pecora and T. L. Carroll, Phys. Rev. A **44**, 2374 (1991).
[27] J.-P. Eckmann and D. Ruelle, Rev. Mod. Phys. **57**, 617 (1985).
[28] J.-P. Eckmann, S. O. Kamphorst, D. Ruelle, and S. Ciliberto, Phys. Rev. A **34**, 4971 (1986).
[29] A. E. Siegman, *Lasers* (University Science Books, Mill Valley, CA, 1986).